Progress In Electromagnetics Research M, Vol. 12, 39–50, 2010

ELECTROMAGNETIC BANDGAP ANALYSIS OF 1D MAGNETIZED PPC WITH OBLIQUE INCIDENCE

L. Yang †**, Y. Xie, P. Yu, and G. Wang**

Department of Communication Enginerring
Jiangsu University
Zhenjiang 212013, China

Abstract—The modified finite-difference time-domain (M-FDTD) method is proposed to analysis electromagnetic bandgap of 1D layered anisotropic plasma photonic crystal (PPC) under the situation of the EM wave oblique incidence. The presence of it avoids the usage of two-dimensional FDTD iterative and greatly improves the computational efficiency. By the algorithm, the reflection coefficients of electromagnetic waves with different incidence angles are computed, and compare the results with the analytical solution. The results show that the method of the accuracy and effectiveness. Finally, the algorithm is applied to calculate electromagnetic bandgap charateristics of PPC with the different incident angles, and their reflection coefficients under the condition of the different incident angles are analyzed.

1. INTRODUCTION

Since the concept of photonic crystal was proposed by John [1] and Yablonovitch [2], due to its own unique characteristics of controlling the flow of light, it has been focused on the optical fields. In addition, due to its own unique characteristics (such as the periodicity of the refractive index, and the characteristic of the forbidden band and pass band), the plasma thus has become the active research topic of the field. So recently Hojo et al. [3] combine the above two together to propose the concept of plasma photonic crystal. Thus it rapidly has become the active research topic of the field. However, the plasma is complex medium which is only dependent on the frequency without the external magnetic, and is also anisotropic with the external magnetic

Corresponding author: L. Yang (lixiayang@yeah.net).
† Also with State Key Laboratory of Millimeter Waves, Southeast University, Nanjing 210096, China.

field. Currently, the finite difference time domain (FDTD) method and transfer matrix method are used to analyze one dimensional (1D) plasma photonic crystal (PPC). By using the transform matrix method in Ref. [4], the dispersion diagram of unmagnetized plasma without collision frequency was only derived, and by the FDTD method in Refs. [5, 6], the features of the PPC with normal incidence were analyzed, and the effect of the incident angle is neglected. In practice, the electromagnetic wave often obliquely illuminates the PPC, so it is important how incident angle effects the bandgap of the PPC in theory and practical application.

In this paper, in order to solve the above problem, a M-FDTD implementation is proposed by which EM wave transmission characteristic can be analyzed for oblique incidence on stratified medium. The FDTD iterative formulas are deduced in the TE and TM wave oblique incidence situation, and the revisions of the connection boundary (CB) and absorbing boundary condition (ABC) in the oblique incidence situation are carried out. By the algorithm, the reflection coefficients of the plasma slab are calculated in the TE and TM wave oblique incidence situation. Finally, the algorithm is applied to calculate electromagnetic scattering by the PPC with the different incident angles, and their reflection coefficients under the condition of the different incident angles are analyzed.

2. M-FDTD ITERATIVE FORMULA IN THE OBLIQUE INCIDENCE SITUATION

Consider a TM_z polarized wave with time factor $e^{j\omega t}$ and the incident angle θ incident from an isotropic medium with permittivity $\varepsilon_1 = \varepsilon_0$ and permeability $\mu_1 = \mu_0$ upon another medium with permittivity ε_2 and permeability μ_2, seen in Fig. 1. We assume the plane of incidence to be parallel to the xoz plane. By the phase-matching conditions the $\mathbf{k}$ vectors of all plane waves will be in the xoz plane. Thus all field vectors will be dependent on x and z only and independent of y. Since $\partial/\partial y = 0$, the Maxwell equations become, in Region 1.

$$\begin{cases} \dfrac{\partial E_x}{\partial z} - \dfrac{\partial E_z}{\partial x} = -\mu_0 j\omega H_y \\ -\dfrac{\partial H_y}{\partial z} = \varepsilon_0 j\omega E_x \\ \dfrac{\partial H_y}{\partial x} = \varepsilon_0 j\omega E_z \end{cases} \tag{1}$$

Taking the partial derivative of the second equation with respect to z and the third one with respect to x, then substituting the results

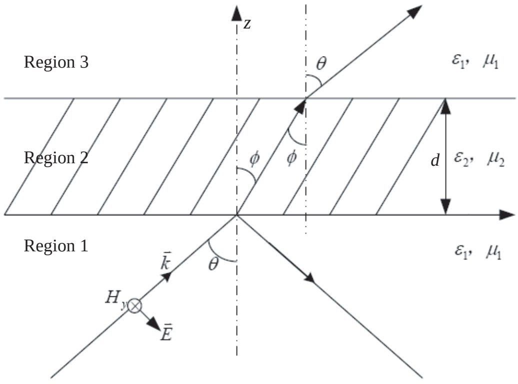

Figure 1. Reflection and transmission of TM waves at a plane boundary separating regions 1 and 2.

into the first one in Eq. (1) system, so we can obtain

$$\frac{\partial^2 H_y}{\partial x^2}+\frac{\partial^2 H_y}{\partial z^2}+\mu_0\varepsilon_0\omega^2 H_y=0 \tag{2}$$

The solution of Eq. (2) can be obtained easily as follows

$$H_y=H_0e^{j(k_x x+k_z z)+j\omega t} \tag{3}$$

So the solution for the 1-D wave propagating in x-direction is

$$\begin{cases} H_{y1D}=H_0e^{jk_x x+j\omega t} \\ E_{z1D}=\dfrac{H_0}{\omega\varepsilon_0}k_x e^{jk_x x+j\omega t} \end{cases} \tag{4}$$

Substituting Eq. (4) into Eq. (1) system and eliminating E_z, then transforming back to the time domain yields

$$\begin{cases} \dfrac{\partial H_{y1D}}{\partial z}=-\varepsilon_0\dfrac{\partial E_{x1D}}{\partial t} \\ \dfrac{k_1^2}{k_{1z}^2}\dfrac{\partial E_{x1D}}{\partial z}=-\mu_0\dfrac{\partial H_{y1D}}{\partial t} \end{cases} \tag{5}$$

where k_1 is wave number in the Region 1, k_{1z} is the z-component of the vector $\vec{k}_1$, and $k_{1z}=k_1\cos\theta$.

By the same procedure of Eq. (5), transforming the 1D modified equations of the Ampere's Law in Region 2 (in the plasma region) to the frequency domain yields

$$\begin{cases} \dfrac{\partial H_{y1D}}{\partial z} = -\varepsilon_2 j\omega E_{x1D} \\ \dfrac{k_2^2}{k_{2z}^2}\dfrac{\partial E_{x1D}}{\partial z} = -\mu_2 j\omega H_{y1D} \end{cases} \tag{6}$$

where k_2 is wave number in the Region 2, k_{2z} is the z-component of $\vec{k}_2$, and $k_{2z} = k_2 \cos\varphi$. Combining the phase-matching conditions and the boundary conditions, we can obtain $k_{1x} = k_{2x}$, $k_{2z}^2 = k_2^2 - k_{2x}^2 = k_2^2 - k_{1x}^2$. Substituting the two equations into the second equation of Eq. (6), finally we can obtain

$$\frac{\partial E_{x1D}}{\partial z} = -j\omega\mu_2 \left(1 - \frac{k_{1x}^2}{k_2^2}\right) H_{y1D} \tag{7}$$

Using $k_x = k\sin\theta$, $k = \omega\sqrt{\varepsilon\mu}$, and assuming

$$\xi_{y1D} = \left(\frac{\varepsilon_{r2} - \varepsilon_{r1}\sin^2\theta}{\varepsilon_{r2}}\right) H_{y1D} \tag{8}$$

Then Eq. (7) yields

$$\frac{\partial E_{x1D}}{\partial z} = -j\omega\mu_2 \xi_{y1D} \tag{9}$$

Substituting Eq. (9) into the second equation of Eq. (6), and combining the results together with Eq. (8), so

$$\begin{cases} \dfrac{\partial H_{y1D}}{\partial z} = -\varepsilon_2 j\omega E_{x1D} \\ \dfrac{\partial E_{x1D}}{\partial z} = -\mu_2 j\omega \xi \\ \xi = \left(\dfrac{\varepsilon_{r2} - \varepsilon_{r1}\sin^2\theta}{\varepsilon_{r2}}\right) H_{y1D} \end{cases} \tag{10}$$

Similarly, E_{y1D}, H_{x1D} have the same formats. Then E_{x1D}, H_{y1D}, E_{y1D}, H_{x1D} are converted to the matrix form as follows

$$\begin{cases} \dfrac{\partial \mathbf{H}}{\partial z} = -\varepsilon_0 \boldsymbol{\varepsilon}_{r2} j\omega \mathbf{E} \\ \dfrac{\partial \mathbf{E}}{\partial z} = -\mu_0 j\omega \boldsymbol{\xi} \\ \boldsymbol{\xi} = \left(\dfrac{\varepsilon_{r2} - \varepsilon_{r1}\sin^2\theta}{\varepsilon_{r2}}\right) \mathbf{H} \end{cases} \tag{11}$$

where $\mathbf{E} = \begin{bmatrix} E_{x1D} \\ E_{y1D} \end{bmatrix}$, $\mathbf{H} = \begin{bmatrix} H_{y1D} \\ H_{x1D} \end{bmatrix}$, $\boldsymbol{\xi} = \begin{bmatrix} \xi_{y1D} \\ \xi_{x1D} \end{bmatrix}$. According to Ref. [7], $\boldsymbol{\varepsilon}_{r2}$ the relative permittivity of the magnetized plasma is

$$\boldsymbol{\varepsilon}_{r2} = \mathbf{I} + \frac{\boldsymbol{\sigma}}{j\omega\varepsilon_0} \tag{12}$$

where $\boldsymbol{\sigma}$ is the conductivity matrix. According to Ref. [8], the constitutive relation for a cold magnetoplasma is given by

$$\frac{d\mathbf{J}}{dt} + v\mathbf{J} = \varepsilon_0\omega_p^2\mathbf{E} + \boldsymbol{\omega}_b \times \mathbf{J} \tag{13}$$

where v is the collision frequency, $\boldsymbol{\omega}_b$ the electron gyrofrequency, ω_p the plasma frequency. Eq. (13) in Cartesian coordinate is expressed as in matrix form.

$$\begin{bmatrix} \dfrac{dJ_x}{dt} \\ \dfrac{dJ_y}{dt} \end{bmatrix} = \varepsilon_0\omega_p^2 \begin{bmatrix} E_x \\ E_y \end{bmatrix} + \boldsymbol{\Omega} \begin{bmatrix} J_x \\ J_y \end{bmatrix} \tag{14}$$

where $\boldsymbol{\Omega} = \begin{pmatrix} -v & -\omega_b \\ \omega_b & -v \end{pmatrix}$. In order to obtain the time-domain $\boldsymbol{\sigma}$ in Eq. (12), we firstly transform Eq. (14) into the frequency domain and obtain $\boldsymbol{\sigma}$ matrix in the frequency-domain according to the Ohm's law $\mathbf{J} = \boldsymbol{\sigma}\mathbf{E}$

$$\boldsymbol{\sigma} = \varepsilon_0\omega_p^2 \left(j\omega\mathbf{I} - \boldsymbol{\Omega}\right)^{-1} = \frac{\varepsilon_0\omega_p^2}{(j\omega + v)^2 + \omega_b^2} \begin{pmatrix} j\omega + v & -\omega_b \\ \omega_b & j\omega + v \end{pmatrix} \tag{15}$$

Then by the IFFT of Eq. (15), $\boldsymbol{\sigma}$ in the time-domain is expressed as, when $v > 0$

$$\boldsymbol{\sigma}(t) = \varepsilon_0\omega_p^2 e^{-vt} \begin{pmatrix} \cos\omega_b t & -\sin\omega_b t \\ \sin\omega_b t & \cos\omega_b t \end{pmatrix} U(t) = \varepsilon_0\omega_p^2 e^{\boldsymbol{\Omega}t} U(t) \tag{16}$$

when $v = 0$

$$\boldsymbol{\sigma}(t) = \frac{\varepsilon_0\omega_p^2}{2} \begin{pmatrix} \cos\omega_b t & -\sin\omega_b t \\ \sin\omega_b t & \cos\omega_b t \end{pmatrix} U(t) = \frac{\varepsilon_0\omega_p^2}{2} e^{\boldsymbol{\Omega}t} U(t) \tag{17}$$

where $U(t)$ is the unit step function.

The FDTD iterative formula under the condition of $v = 0$ is similar to $v > 0$, so we only derive the FDTD iterative formula under the condition of $v > 0$. Substituting Eq. (12) and Eq. (16) into Eq. (11), then transform the results into the time domain. We can obtain

$$\begin{cases} \dfrac{\partial \mathbf{H}}{\partial z} = -\varepsilon_0 \dfrac{\partial \mathbf{E}}{\partial t} - \boldsymbol{\sigma}(t) * \mathbf{E} \\ \dfrac{\partial \mathbf{E}}{\partial z} = -\mu_0 \dfrac{\partial \boldsymbol{\xi}}{\partial t} \\ \dfrac{\partial \boldsymbol{\xi}}{\partial t} = \left(\varepsilon_{r2} - \varepsilon_{r1}\sin^2\theta\right) \dfrac{\partial \mathbf{H}}{\partial t} + \dfrac{1}{\varepsilon_0} \left[\boldsymbol{\sigma}(t) * \mathbf{H}(t) - \boldsymbol{\sigma}(t) * \boldsymbol{\xi}(t)\right] \end{cases} \tag{18}$$

Assuming

$$\begin{cases} \boldsymbol{\varphi}(t) = e^{\boldsymbol{\Omega} t} U(t) * \mathbf{E}(t) \\ \boldsymbol{\chi}(t) = e^{\boldsymbol{\Omega} t} U(t) * \boldsymbol{\xi}(t) \\ \boldsymbol{\psi}(t) = e^{\boldsymbol{\Omega} t} U(t) * \mathbf{H}(t) \end{cases} \tag{19}$$

and by the JE convolution (JEC) method in Ref. [9], the convolutions in Eq. (19) system can be deduced, then the FDTD iterative formula of Eq. (18) and Eq. (19) can be obtained

$$\boldsymbol{\xi}^{n+\frac{1}{2}}\left(k+\frac{1}{2}\right) = \boldsymbol{\xi}^{n-\frac{1}{2}}\left(k+\frac{1}{2}\right) - \frac{\Delta t}{\mu_0 \Delta z}\left[\mathbf{E}^n(k+1) - \mathbf{E}^n(k)\right] \tag{20}$$

$$\begin{aligned} \mathbf{H}^{n+\frac{1}{2}}\left(k+\frac{1}{2}\right) = {} & \mathbf{H}^{n-\frac{1}{2}}\left(k+\frac{1}{2}\right) + \frac{1}{\varepsilon_{r2} - \varepsilon_{r1}\sin^2\theta} \\ & \left[\boldsymbol{\xi}^{n+\frac{1}{2}}\left(k+\frac{1}{2}\right) - \boldsymbol{\xi}^{n-\frac{1}{2}}\left(k+\frac{1}{2}\right)\right] \\ & + \frac{\Delta t \omega_p^2}{\varepsilon_{r2} - \varepsilon_{r1}\sin^2\theta}\left[\boldsymbol{\chi}^n\left(k+\frac{1}{2}\right) - \boldsymbol{\psi}^n\left(k+\frac{1}{2}\right)\right] \end{aligned} \tag{21}$$

$$\begin{aligned} \boldsymbol{\chi}^n\left(k+\frac{1}{2}\right) = {} & e^{-v\Delta t}\begin{pmatrix} \cos\omega_b\Delta t & -\sin\omega_b\Delta t \\ \sin\omega_b\Delta t & \cos\omega_b\Delta t \end{pmatrix} \boldsymbol{\chi}^{n-1}\left(k+\frac{1}{2}\right) \\ & + \Delta t \cdot e^{-\frac{v\Delta t}{2}} \begin{pmatrix} \cos\left(\frac{\omega_b \Delta t}{2}\right) & -\sin\left(\frac{\omega_b \Delta t}{2}\right) \\ \sin\left(\frac{\omega_b \Delta t}{2}\right) & \cos\left(\frac{\omega_b \Delta t}{2}\right) \end{pmatrix} \\ & \boldsymbol{\xi}^{n-\frac{1}{2}}\left(k+\frac{1}{2}\right) \end{aligned} \tag{22}$$

$$\begin{aligned} \boldsymbol{\psi}^n\left(k+\frac{1}{2}\right) = {} & e^{-v\Delta t}\begin{pmatrix} \cos\omega_b\Delta t & -\sin\omega_b\Delta t \\ \sin\omega_b\Delta t & \cos\omega_b\Delta t \end{pmatrix} \boldsymbol{\psi}^{n-1}\left(k+\frac{1}{2}\right) \\ & + \Delta t \cdot e^{-\frac{v\Delta t}{2}} \begin{pmatrix} \cos\left(\frac{\omega_b \Delta t}{2}\right) & -\sin\left(\frac{\omega_b \Delta t}{2}\right) \\ \sin\left(\frac{\omega_b \Delta t}{2}\right) & \cos\left(\frac{\omega_b \Delta t}{2}\right) \end{pmatrix} \\ & \mathbf{H}^{n-\frac{1}{2}}\left(k+\frac{1}{2}\right) \end{aligned} \tag{23}$$

$$\begin{aligned} \mathbf{E}^{n+1}(k) = {} & \mathbf{E}^n(k) - \frac{1}{\varepsilon_0}\frac{\Delta t}{\Delta z}\left[\mathbf{H}^{n+\frac{1}{2}}\left(k+\frac{1}{2}\right) - \mathbf{H}^{n+\frac{1}{2}}\left(k-\frac{1}{2}\right)\right] \\ & - \Delta t \omega_p^2 \boldsymbol{\varphi}^{n+\frac{1}{2}}(k) \end{aligned} \tag{24}$$

$$\boldsymbol{\varphi}^n\left(k+\frac{1}{2}\right) = e^{-v\Delta t}\begin{pmatrix} \cos\omega_b\Delta t & -\sin\omega_b\Delta t \\ \sin\omega_b\Delta t & \cos\omega_b\Delta t \end{pmatrix} \boldsymbol{\varphi}^{n-1}\left(k+\frac{1}{2}\right)$$

$$+\Delta t \cdot e^{-\frac{v\Delta t}{2}} \begin{pmatrix} \cos\left(\frac{\omega_b \Delta t}{2}\right) & -\sin\left(\frac{\omega_b \Delta t}{2}\right) \\ \sin\left(\frac{\omega_b \Delta t}{2}\right) & \cos\left(\frac{\omega_b \Delta t}{2}\right) \end{pmatrix}$$
$$\mathbf{E}^{n-\frac{1}{2}}\left(k+\frac{1}{2}\right) \tag{25}$$

Similarly, the FDTD iterative formula of the TE_z polarized wave is

$$\mathbf{H}^{n+1/2}\left(k+\frac{1}{2}\right) = \mathbf{H}^{n-1/2}\left(k+\frac{1}{2}\right) - \frac{\Delta t}{\mu_0 \Delta z}\left[\mathbf{E}^n(k+1) - \mathbf{E}^n(k)\right] \tag{26}$$

$$\begin{aligned} \mathbf{E}^{n+1}(k) &= \mathbf{E}^n(k) - \frac{\Delta t}{\varepsilon_0\left(\varepsilon_{r2} - \varepsilon_{r1}\sin^2\theta\right)\Delta z} \\ &\quad \left[\mathbf{H}^{n+1/2}\left(k+\frac{1}{2}\right) - \mathbf{H}^{n+1/2}\left(k-\frac{1}{2}\right)\right] \\ &\quad + \frac{\omega_p^2 \Delta t}{\varepsilon_{r2} - \varepsilon_{r1}\sin^2\theta} \boldsymbol{\chi}^{n+\frac{1}{2}}(k) \end{aligned} \tag{27}$$

$$\begin{aligned} \boldsymbol{\chi}^n\left(k+\frac{1}{2}\right) &= e^{-v\Delta t}\begin{pmatrix} \cos\omega_b\Delta t & -\sin\omega_b\Delta t \\ \sin\omega_b\Delta t & \cos\omega_b\Delta t \end{pmatrix} \boldsymbol{\chi}^{n-1}\left(k+\frac{1}{2}\right) \\ &\quad + \Delta t \cdot e^{-\frac{v\Delta t}{2}} \begin{pmatrix} \cos\left(\frac{\omega_b \Delta t}{2}\right) & -\sin\left(\frac{\omega_b \Delta t}{2}\right) \\ \sin\left(\frac{\omega_b \Delta t}{2}\right) & \cos\left(\frac{\omega_b \Delta t}{2}\right) \end{pmatrix} \\ &\quad \mathbf{E}^{n-\frac{1}{2}}\left(k+\frac{1}{2}\right) \end{aligned} \tag{28}$$

where $\mathbf{E} = \begin{bmatrix} E_{x1D} \\ E_{y1D} \end{bmatrix}$, $\mathbf{H} = \begin{bmatrix} H_{y1D} \\ H_{x1D} \end{bmatrix}$, $\boldsymbol{\chi} = \begin{bmatrix} \boldsymbol{\chi}_{x1D} \\ \boldsymbol{\chi}_{y1D} \end{bmatrix}$.

3. REVISION OF MUR ABC AND CB

3.1. Revision of Mur ABC

In the FDTD computation, Mur ABC is employed. Under the condition of the oblique incidence in the free space, Mur ABCs are revised as follows:

$$\text{Left Mur ABC:} \quad E^{n+1}(k) = E^n(k+1) + \frac{cdt - dz\cos\theta}{cdt + dz\cos\theta}\left[E^{n+1}(k+1) - E^n(k)\right] \tag{29}$$

$$\text{Right Mur ABC:} \quad E^{n+1}(k) = E^n(k-1) + \frac{cdt - dz\cos\theta}{cdt + dz\cos\theta}\left[E^{n+1}(k-1) - E^n(k)\right] \tag{30}$$

3.2. Revision of CB

Based on the CB theory in Ref. [10], under the condition of the oblique incidence in the free space, CBs are also revised as follows

$$\mathrm{TE}_z: \begin{cases} E^{n+1}(k_0) = E^{n+1}(k_0)_{\mathrm{FDTD}} + \dfrac{\Delta t}{\varepsilon_0 \Delta z \cos^2\theta} H_i^{n+\frac{1}{2}}\left(k_0 - \dfrac{1}{2}\right) \\ H^{n+\frac{1}{2}}\left(k_0 - \dfrac{1}{2}\right) = H^{n-\frac{1}{2}}\left(k_0 - \dfrac{1}{2}\right)_{\mathrm{FDTD}} + \dfrac{\Delta t}{\mu_0 \Delta z} E_i^n(k_0) \end{cases} \tag{31}$$

$$\mathrm{TM}_z: \begin{cases} E^{n+1}(k_0) = E^{n+1}(k_0)_{\mathrm{FDTD}} + \dfrac{\Delta t}{\varepsilon_0 \Delta z} H_i^{n+\frac{1}{2}}\left(k_0 - \dfrac{1}{2}\right) \\ H^{n+\frac{1}{2}}\left(k_0 - \dfrac{1}{2}\right) = H^{n-\frac{1}{2}}\left(k_0 - \dfrac{1}{2}\right)_{\mathrm{FDTD}} + \dfrac{\Delta t}{\mu_0 \Delta z \cos^2\theta} E_i^n(k_0) \end{cases} \tag{32}$$

4. VALIDATION OF MODIFIED FDTD ALGORITHM

In order to validate the accuracy of the above algorithm, we simulate the transient propagation of the TE_z and TM_z polarized wave that is obliquely incident with $\theta = \frac{\pi}{6}, \frac{\pi}{4}, \frac{\pi}{3}$ on a magnetized plasma slab with a thickness of 15.0 mm. The incident wave used in the simulation is a Gaussian-derivative pulsed plane wave whose frequency spectrum peaks at 50 GHz and is 10 dB down from the peak at 100 GHz. The plasma parameters are $v = 20$ GHz, $\omega_b = 100$ GHz, $\omega_p = 28.7$ GHz, The spatial discretization, Δz, used in the simulations is 75 μm and the time step $\Delta t = \Delta z/2c$, is 0.125 ps, both ends of the computed space are applied by the revision of Mur ABCs. In Figs. 2(a) and (b), the reflection coefficients of the right circular polarization (RCP) of TM_z and TE_z waves by using the M-FDTD algorithm are compared with those of the analytical solution. From the two figures, the FDTD method is in agreement with the analytical solution for the reflection coefficients.

5. BANDGAP ANALYSIS OF MAGNETIZED PPC FOR OBLIQUE INCIDENCE

In Fig. 3, the plane wave illuminates on 1D PPC with θ incident angle, and the thicknesses of dielectric and plasma slab are both 200 grids, and the relative permittivity in dielectric is $\varepsilon_r = 4$. The incident source, spatial discretization and time step are all the same as the validation example.

Example 1: Bandgap analysis under the condition of the different oblique incident angle for the magnetized PPC. The parameters in

FDTD computation are $\theta = 0$, $\frac{\pi}{6}$, $\frac{\pi}{4}$, $\frac{\pi}{3}$ and $v = 20\,\text{GHz}$, $\omega_p = 20\,\text{GHz}$, $\omega_b = 100\,\text{GHz}$. The reflection coefficients of the TM_z and TE_z wave are given in Fig. 4 and Fig. 5.

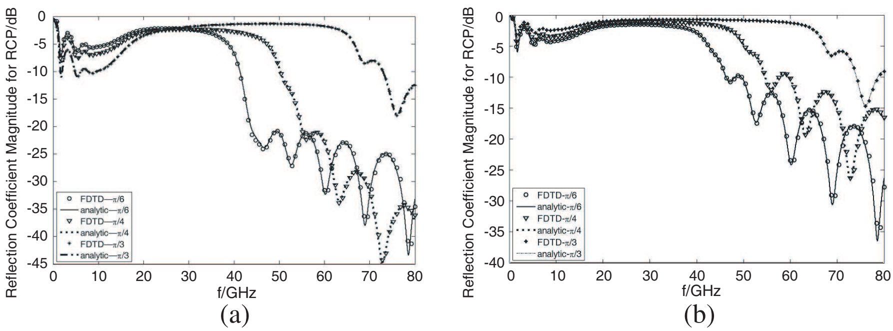

Figure 2. Reflection coefficient magnitude of the RCP wave for $\theta = \frac{\pi}{6}$, $\frac{\pi}{4}$, $\frac{\pi}{3}$. (a) TM_z. (b) TE_z.

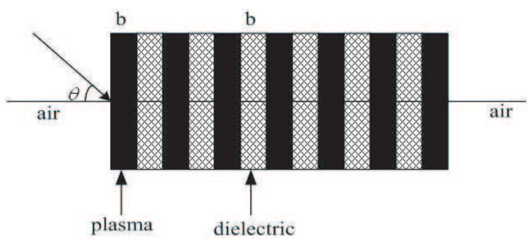

Figure 3. The PPC in the oblique incidence.

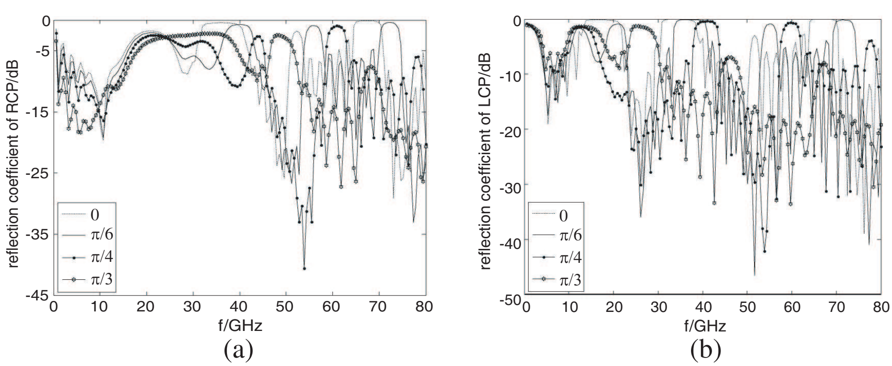

Figure 4. Reflection coefficient magnitude of the TM_z polarized wave with $\theta = 0$, $\frac{\pi}{6}$, $\frac{\pi}{4}$, $\frac{\pi}{3}$. (a) RCP wave. (b) LCP wave.

From Figs. 4(a) and (b), we can see that for TM_z wave, the little the incident angle is, the more significant the periodicity of the band-gap is. When the incident angle is enough large, the band-gap of the photonic crystals vanish. However, for TE_z wave, the band-gap increase and the center frequency move into the high frequency with the increasing of the incident angle. So in order to increase the width of the band-gap, different measures are adopted for different polarizations.

Example 2: Bandgap analysis under the condition of the different oblique incident angle for the unmagnetized PPC. The parameters in FDTD computation are $\theta = 0, \frac{\pi}{6}, \frac{\pi}{4}, \frac{\pi}{3}$ and $v = 20\,\text{GHz}$, $\omega_p = 20\,\text{GHz}$, $\omega_b = 0\,\text{GHz}$. The reflection coefficients of the TM_z and TE_z polarized wave are given in Fig. 6.

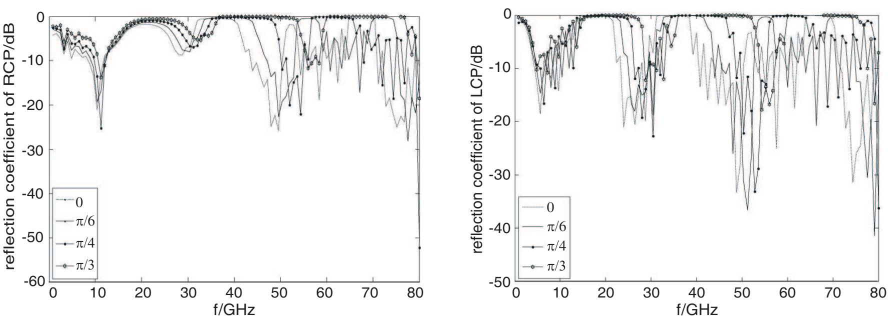

(a) (b)

Figure 5. Reflection coefficient magnitude of the TE_z polarized wave with $\theta = 0, \frac{\pi}{6}, \frac{\pi}{4}, \frac{\pi}{3}$. (a) RCP wave. (b) LCP wave.

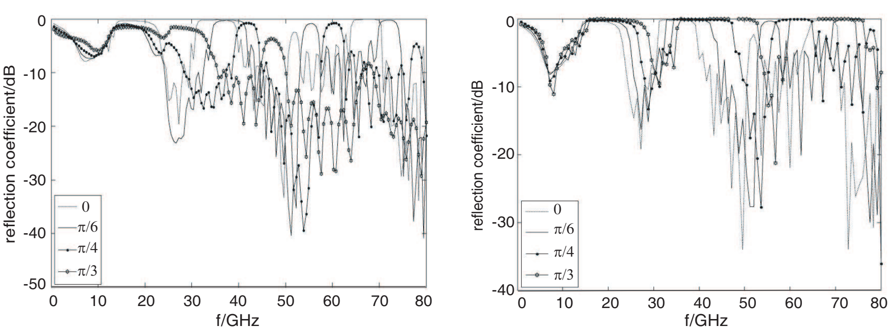

(a) (b)

Figure 6. Reflection coefficients magnitude for $\theta = 0, \frac{\pi}{6}, \frac{\pi}{4}, \frac{\pi}{3}$. (a) TM_z. (b) TE_z.

From Fig. 6(a), we conclude that unmagnetized PPCs are similar to magnetized PPCs. For TM_z wave, the little the incident angle is, the more significant the periodicity of the band-gap is. However, for TE_z wave, from Fig. 6(b), the band-gap increase and the center frequency of it move into the high frequency with the increase of the incident angle. So in order to increase the width of the band-gap, different measures are adopted for different polarizations.

6. CONCLUSION

In this paper, a modified FDTD implementation is proposed by which EM wave transmission characteristic can be analyzed for oblique incidence on 1D PPCs. This method transforms two-dimensional electromagnetic wave transmission question to one-dimensional one, FDTD iterative formulas are deduced in the TE and TM wave oblique incidence situation, and the revisions of the CB and ABC in the oblique incidence situation are carried out. The EM wave reflection coefficients of the plasma slab are calculated in the TE and TM wave oblique incidence situation. The computed results and analytic solutions are in good agreement. The computed results indicate the accuracy and validity of this method. Finally, the algorithm is applied to calculate electromagnetic scattering by the PPCs with the different incident angles, and their bandgap charecteristics under the condition of the different incident angles are analyzed.

ACKNOWLEDGMENT

The authors would like to acknowledge the financial support from the Ph.D. Programs Foundation of Ministry of Education of China (Grand No. 20093227120018), the Science and Techniques Planning Project of Jiangsu province (Grand No. BE2008107), the Openning Funding of the State Key Laboratory of Millimeter Waves (Grand No. K200910), and the Advanced Professional Scientific Research Foundation of Jiangsu University (Grand No. 07JDG063).

REFERENCES

1. John, S., "Strong localization of photons in certain disordered dielectric superlattices," *Phys. Rev. Lett.*, Vol. 58, No. 20, 2486–2489, 1987.
2. Yablonovitch, E., "Inhibited spontaneous emission in solid-state physics and electronics," *Phys. Rev. Lett.*, Vol. 58, No. 23, 2059–2060, 1987.

3. Hojo, H. and A. Mase, "Dispersion relation of electromagnetic wave in one-dimensional plasma photonic crystals," *Plasma Fusion Res.*, Vol. 80, 89, 2004.
4. Guo, B., "Transfer matrix for obliquely incident electromagnetic waves propagating in one dimension plasma photonic crystals," *Plasma Science and Technology*, Vol. 11, No. 1, 19–22, 2009.
5. Liu, S. B., C. Q. Gu, and J. J. Zhou, "FDTD simulation for magnetized plasma photonic crystals," *Acta Physica Sinica*, Vol. 55, No. 3, 1283–1289, 2006 (in Chinese).
6. Liu, S., W. Hong, and N. Yuan, "Finite-difference time-domain analysis of unmagnetized plasma photonic crystals," *International Journal of Infrared and Millimeter Waves*, Vol. 27, No. 3, 403–423, 2006.
7. Dikshitulu, K. K., *Electromagnetics of Complex Media*, CRC Press, 1999.
8. Ginzberg, V. L., *The Propagation of Electromagnetic Waves in Plasma*, Pergammon Press, New York, 1970.
9. Chen, Q., M. Katsurai, and P. H. Aoyagi, "An FDTD formulation for dispersive media using a current density," *IEEE Trans. Antennas Propagat.*, Vol. 46, No. 10, 1739–1746, 1998.
10. Taflove, A. and S. C. Hagness, *Computational Electrodynamics: The Finite-difference Time-domain Method*, 3rd edition, Artech House, Boston, 2005.